



Imaging in COVID-19 complications

**M.Soltani.MD.Radiologist
Assistant professor of Zanzan
University of Medical Science**

- commonly reported sequelae are:
- [acute respiratory distress syndrome \(ARDS\)](#): ~22.5% (range 17-29%)⁸⁹
- acute thromboembolic disease¹³⁰
 - [pulmonary embolism](#)^{114,117,131-133}
 - [deep vein thrombosis \(DVT\)](#)¹²³
- acute cardiac injury: [elevated troponin levels](#)²¹⁰
 - up to 30% of COVID-19 cases that have been hospitalized, with rates exceeding 50% in those with a prior cardiac history
 - [myocardial ischemia](#)
 - [myocarditis](#)¹²⁰
 - [arrhythmias](#)
 - [cardiomyopathy](#)
 - [cardiogenic shock](#)
 - [cardiac arrest](#)
 - [heart failure](#)²¹³

- CNS

- [delirium](#) (15%) ^{137,210}
- [viral encephalitis](#) ¹²¹
- diffuse leukoencephalopathy ¹⁵⁷
- [microhemorrhage](#) ¹⁵⁷⁻¹⁵⁹
 - juxtacortical white matter and corpus callosum (particularly of the splenium)
- [stroke](#) (6%): cryptogenic/ischemic ^{150,151,210}
 - higher mortality and greater severity of stroke in context of COVID-19 ¹⁵⁰
- [Guillain-Barré syndrome \(GBS\)](#): rare ¹⁸²

- secondary infections, e.g. [bacterial pneumonia](#), [mucormycosis](#) ²¹⁵
- [sepsis](#)
- renal ²¹⁰
 - [acute kidney injury \(AKI\)](#) (20-40% of hospitalized patients) ²¹⁰
 - [interstitial](#) and/or [hemorrhagic cystitis](#)
- [coagulopathy](#) ¹⁴⁴
 - [disseminated intravascular coagulation \(DIC\)](#)

- Hepatobiliary:
- liver is the most frequently affected organ after the lungs, although serious sequelae are rare ²¹⁰fulminant liver failure is rare
- portal vein thrombosis
- hepatic vein thrombosis
- acute cholecystitis: due to biliary stasis

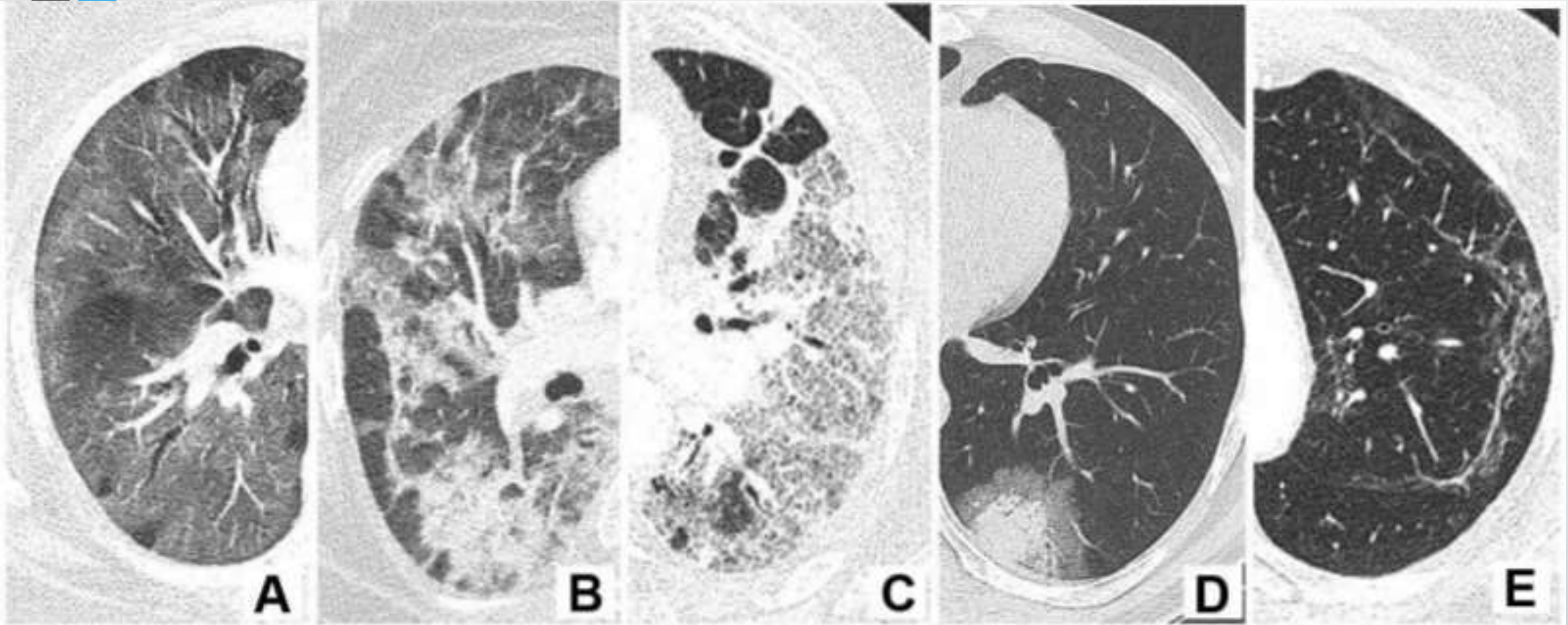
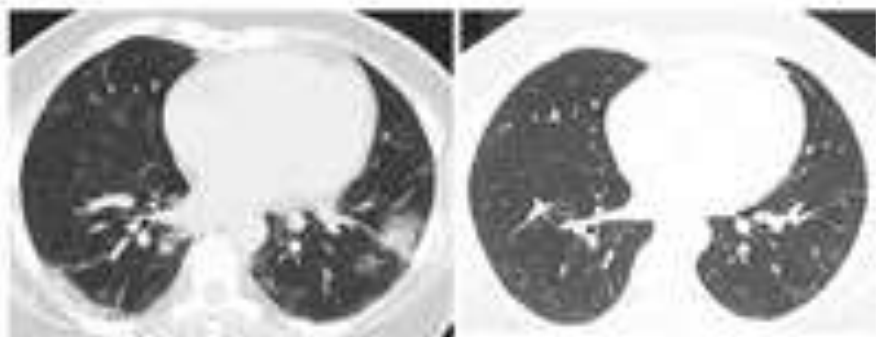


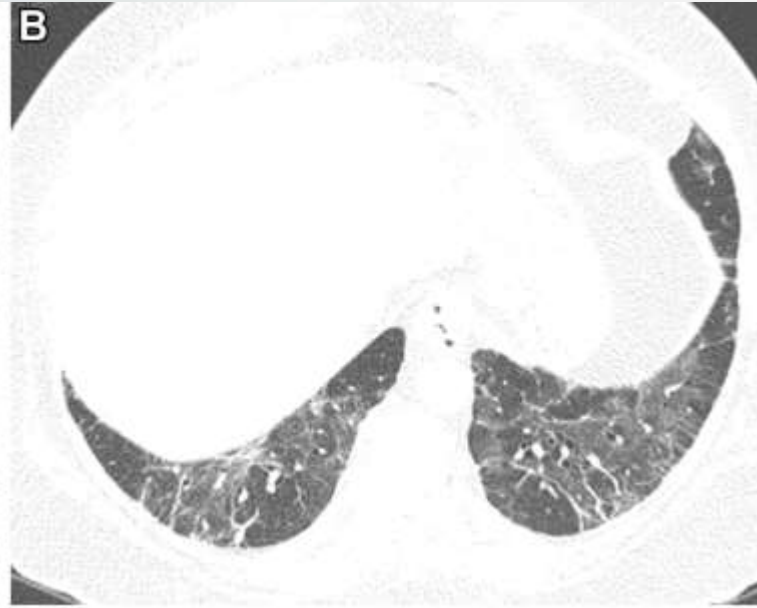
Figure 1: Typical chest CT patterns of COVID-19 viral involvement: a. Ground-glass opacities. b. Consolidations. c. Cobblestone pattern. d. Halo sign. e. Subpleural bands.

CT of Post-Acute Lung Complications of COVID-19

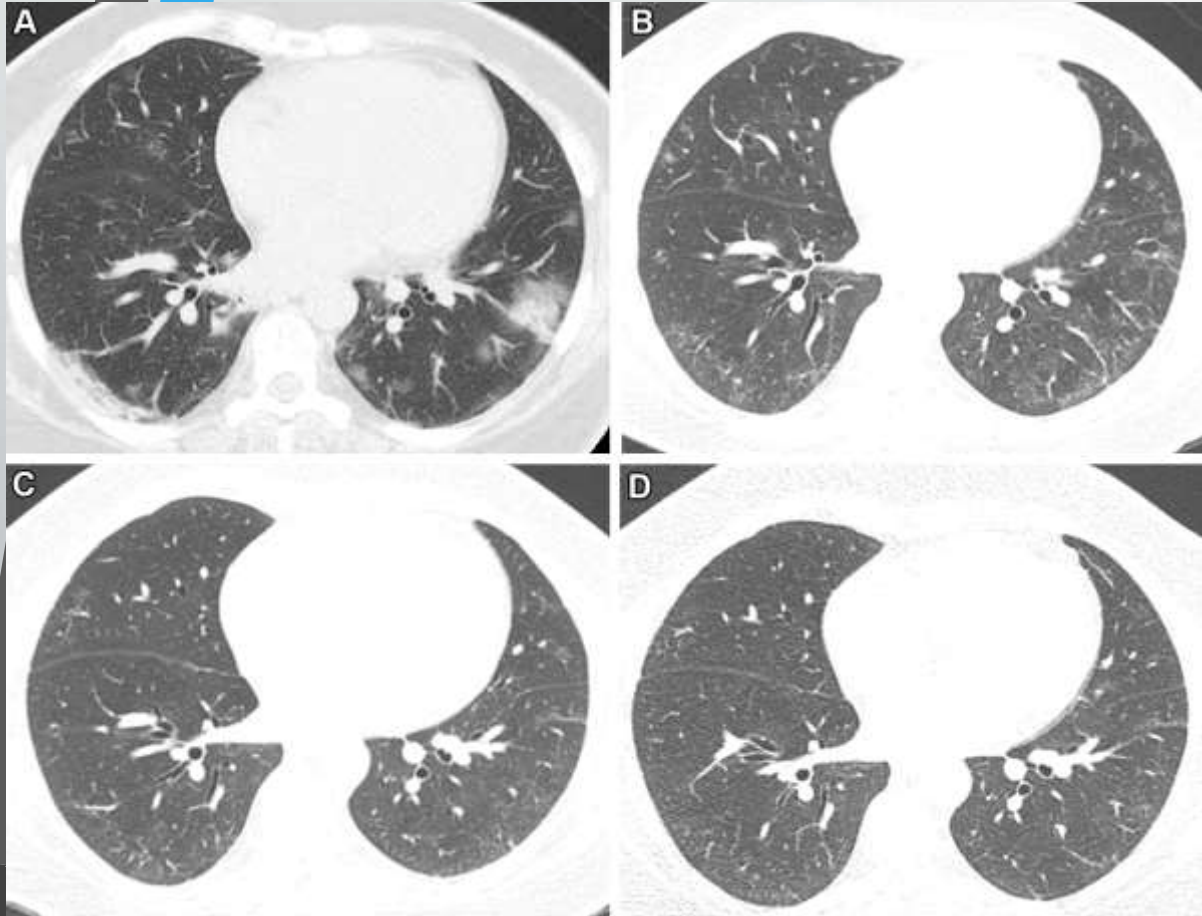


Images in a 59-year-old woman with sequelae of COVID-19–related acute respiratory distress syndrome. Left: CT on admission shows patchy nodular consolidation. Right: Eleven months later, there is still mild residual GGO, but symptoms had resolved and pulmonary function test was normal.

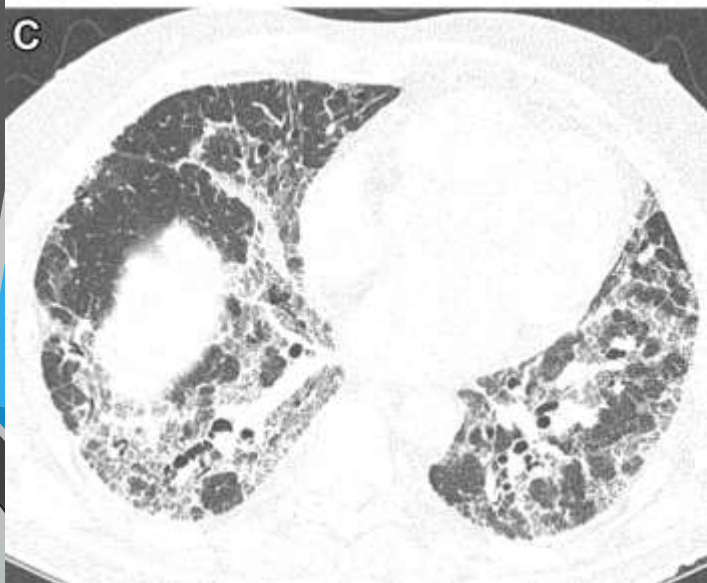
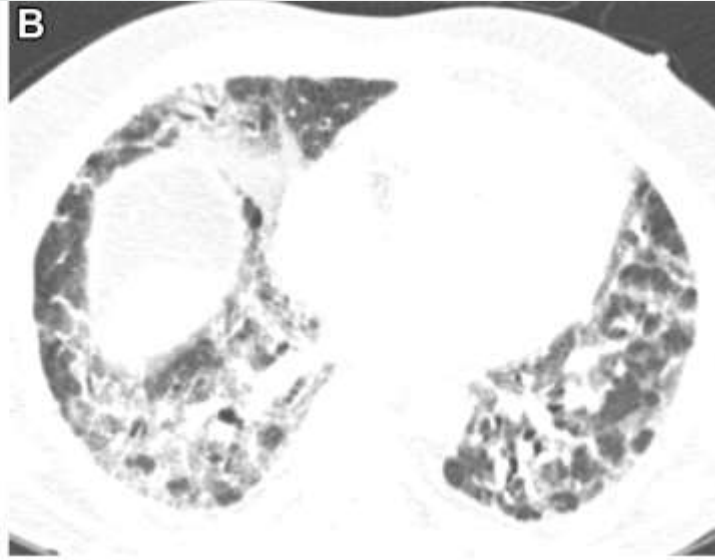
- More than 50% of previously hospitalized survivors of SARS-CoV-2 infection will have abnormality at CT, more commonly in those with more severe acute infection.
- The most common abnormalities are ground-glass opacity (GGO), parenchymal or subpleural bands, reticular abnormality, evidence of fibrotic abnormality, and air trapping.
- Precise radiologic description is important; the term *fibrosis* should be reserved for those with clear evidence of fibrosis (traction bronchiectasis or bronchiolectasis, honeycombing, or architectural distortion).



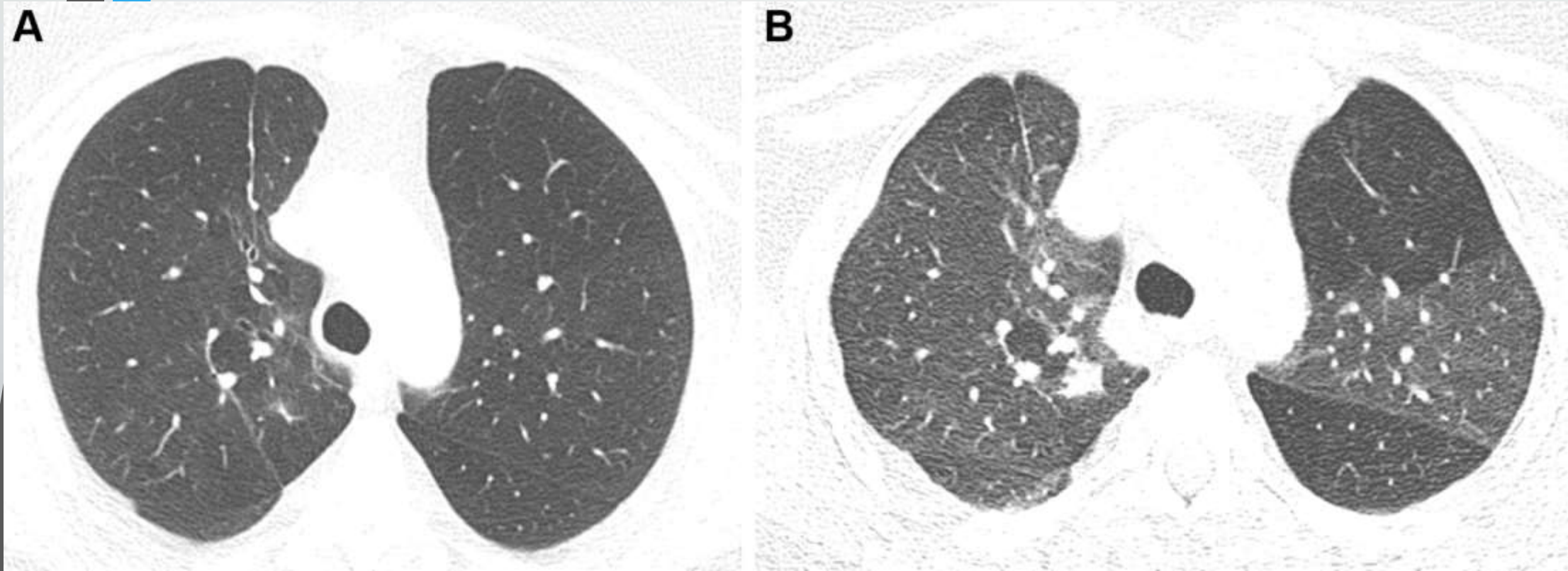
images in a 59-year-old woman with sequelae of COVID-19-related acute respiratory distress syndrome (ARDS). (A) Axial CT on admission shows patchy consolidation and ground-glass opacity (GGO). This subsequently progressed to ARDS. (B) Two months later, consolidation has resolved but there is moderate GGO, multifocal linear abnormality, and mild bronchiectasis. (C) Seven months after admission, these abnormalities had almost completely resolved, and restrictive pulmonary function also resolved.



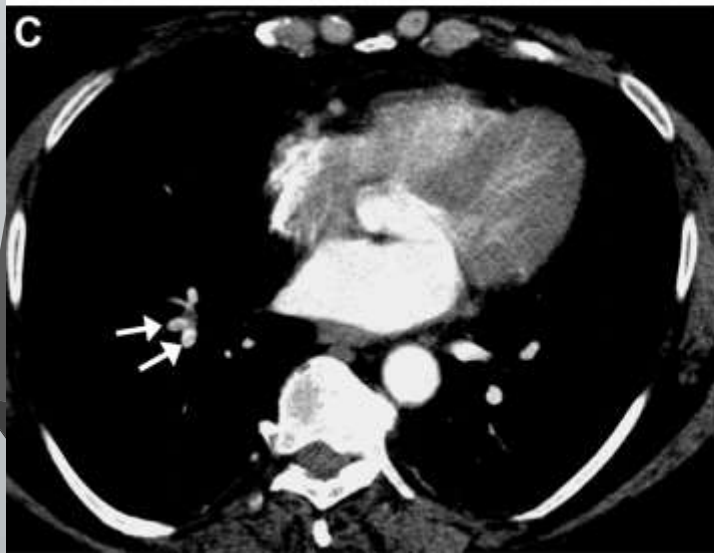
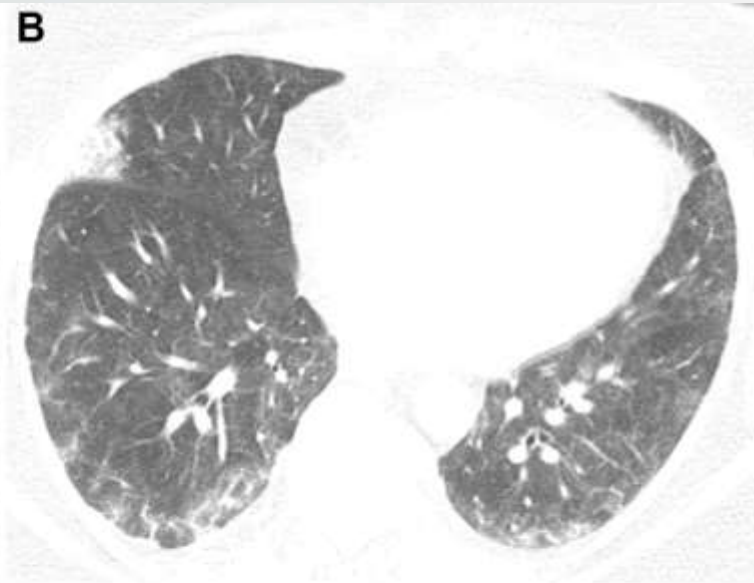
images in a 59-year-old woman with sequelae of COVID-19-related acute respiratory distress syndrome (ARDS). (A) Axial CT on admission shows patchy nodular consolidation. Halo of ground-glass opacity (GGO) is present around largest left lower lobe nodule. Patient subsequently developed ARDS. (B) Two months later, consolidation has resolved with moderate GGO. (C) Three months after admission, there is further improvement in ground glass. (D) Eleven months after admission, there is still mild residual GGO, but symptoms had resolved and pulmonary function test was normal.



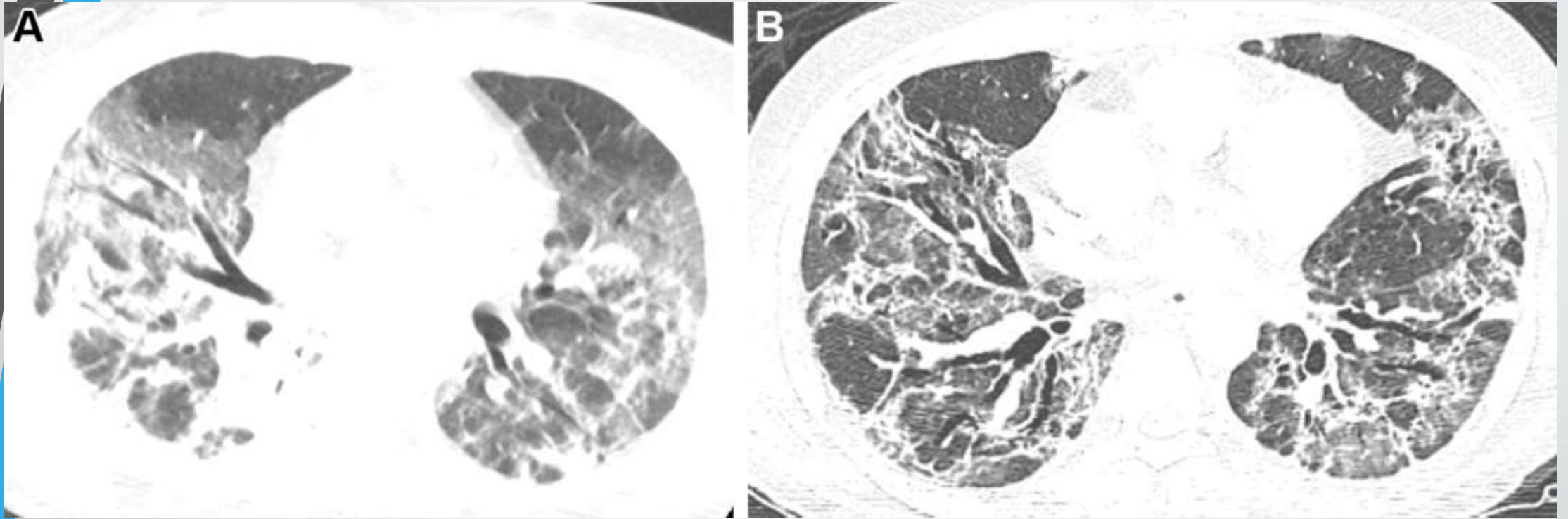
Images show progressive pulmonary fibrosis in a 67-year-old man with a history of relatively mild, stable, fibrotic hypersensitivity pneumonitis. (A) Baseline axial CT shows mild ground-glass and reticular abnormality. (B) Axial CT angiogram obtained 2 months after infection shows substantially increased reticular abnormality with mild traction bronchiectasis. (C) Axial CT obtained 2 months later shows increased traction bronchiectasis indicating progressive fibrosis.



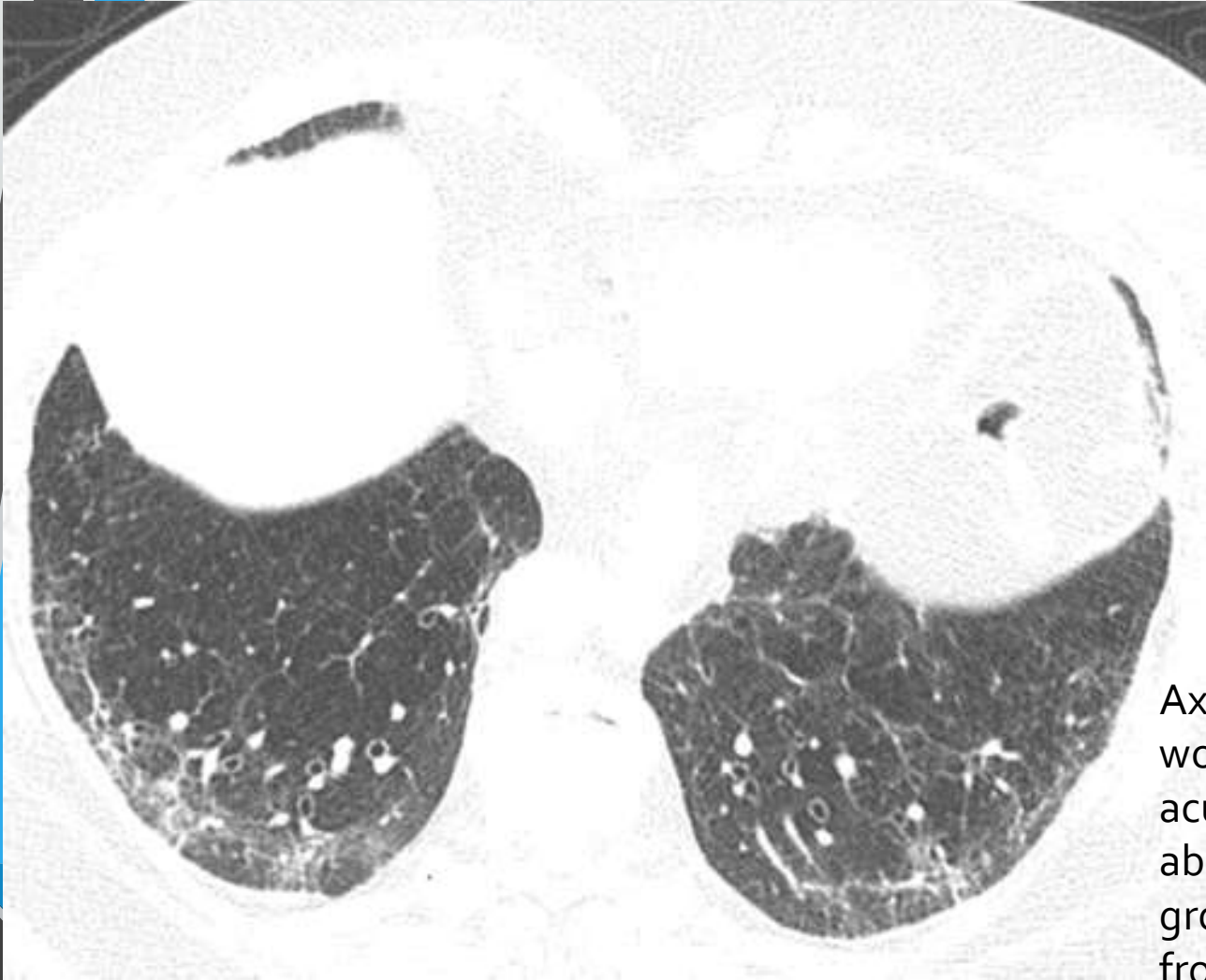
Images demonstrate obstructive lung disease after COVID-19 in a 60-year-old woman. (A) Axial inspiratory CT with persistent shortness of breath and chest tightness 8 months following COVID-19 infection shows subtle mosaic attenuation, best seen in anterior left upper lobe. (B) Axial expiratory CT confirms lobular air trapping, which was present on multiple images, indicating small airway obstruction.



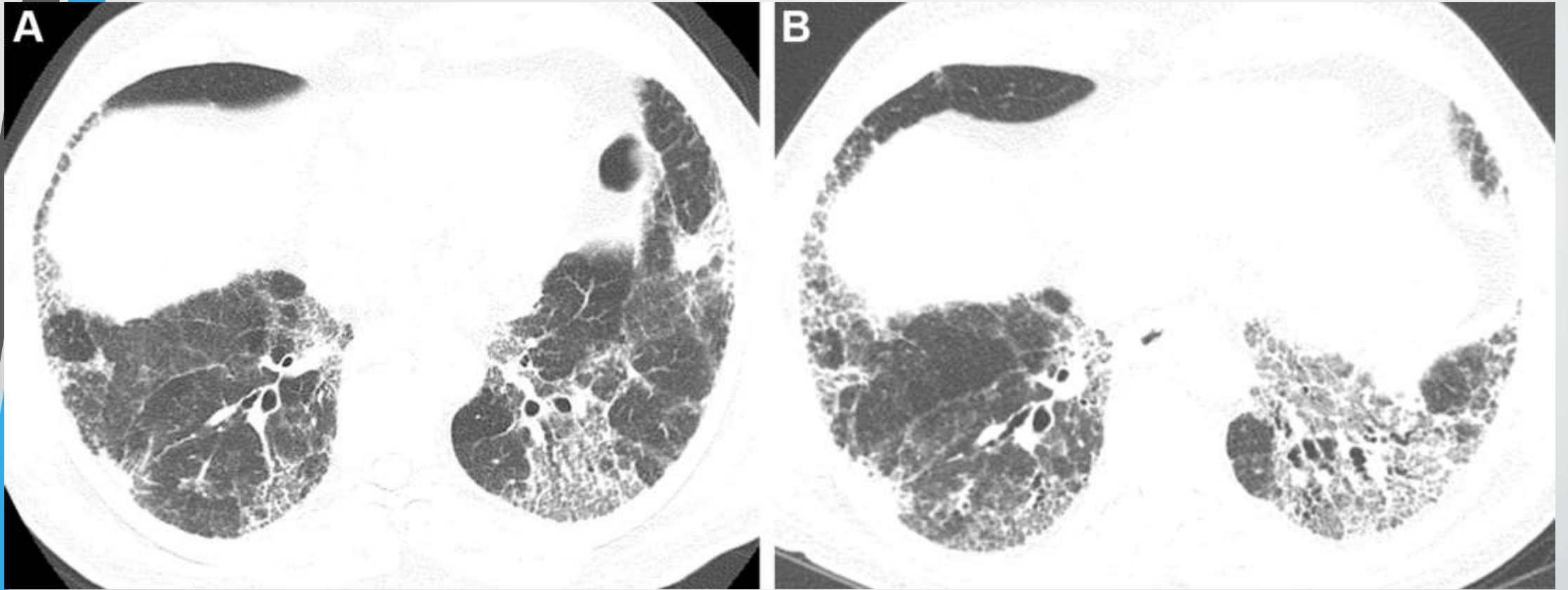
Images depict pulmonary vascular disease after COVID-19 in a 63-year-old woman with persistent shortness of breath and elevated D-dimer level. (A) Axial CT pulmonary arteriogram with persistent shortness of breath and elevated D-dimer level, 7 weeks after onset of infection, shows obstructive thrombus in right interlobar pulmonary artery. (B) Axial CT with lung windows at lower level shows patchy ground-glass opacity and focal wedge-shaped consolidative abnormality in right middle lobe, typical for pulmonary infarct. (C) Three months later, large central thrombus had resolved, but nonocclusive linear webs were present in segmental vessels (arrows), typical for chronic thromboembolic disease.



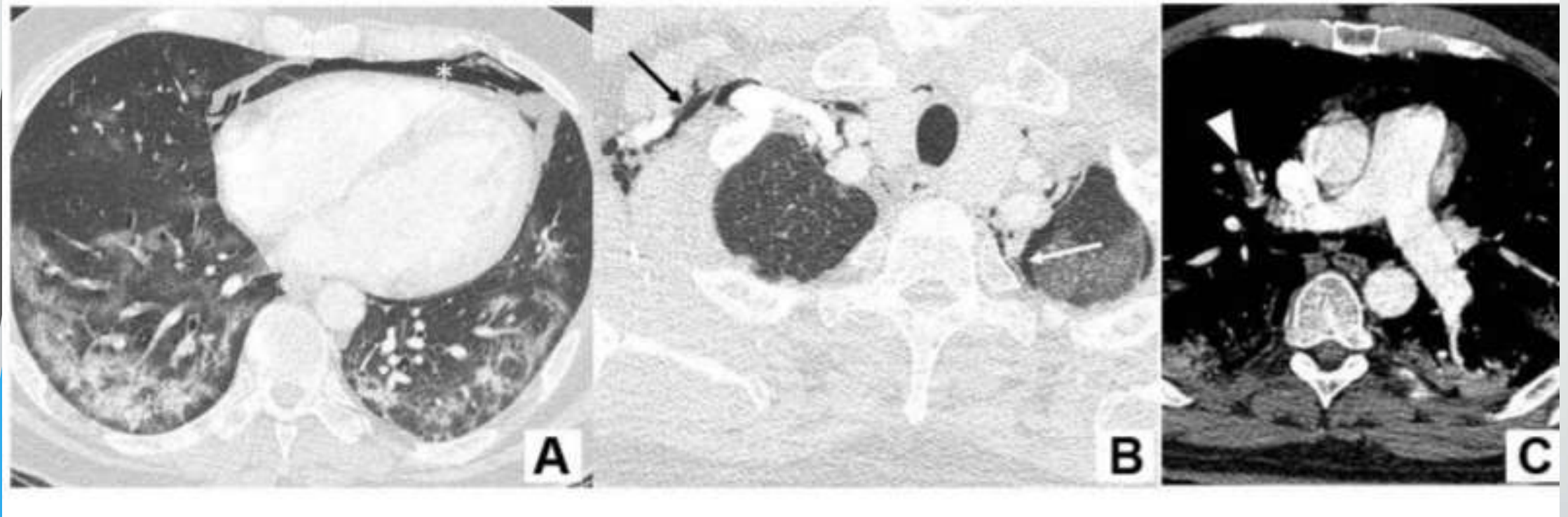
Images in a 54-year-old man with COVID-19–related acute respiratory distress syndrome and subsequent fibrosis. (A) Axial CT 2 weeks after admission shows diffuse ground-glass opacity (GGO) with reticular abnormality and traction bronchiectasis in right middle lobe, indicating organizing phase of lung injury. (B) Axial CT 6 months after admission shows decreased GGO but extensive traction bronchiectasis and architectural distortion, suggesting fibrosis. Patient remained symptomatic with restricted pulmonary function.



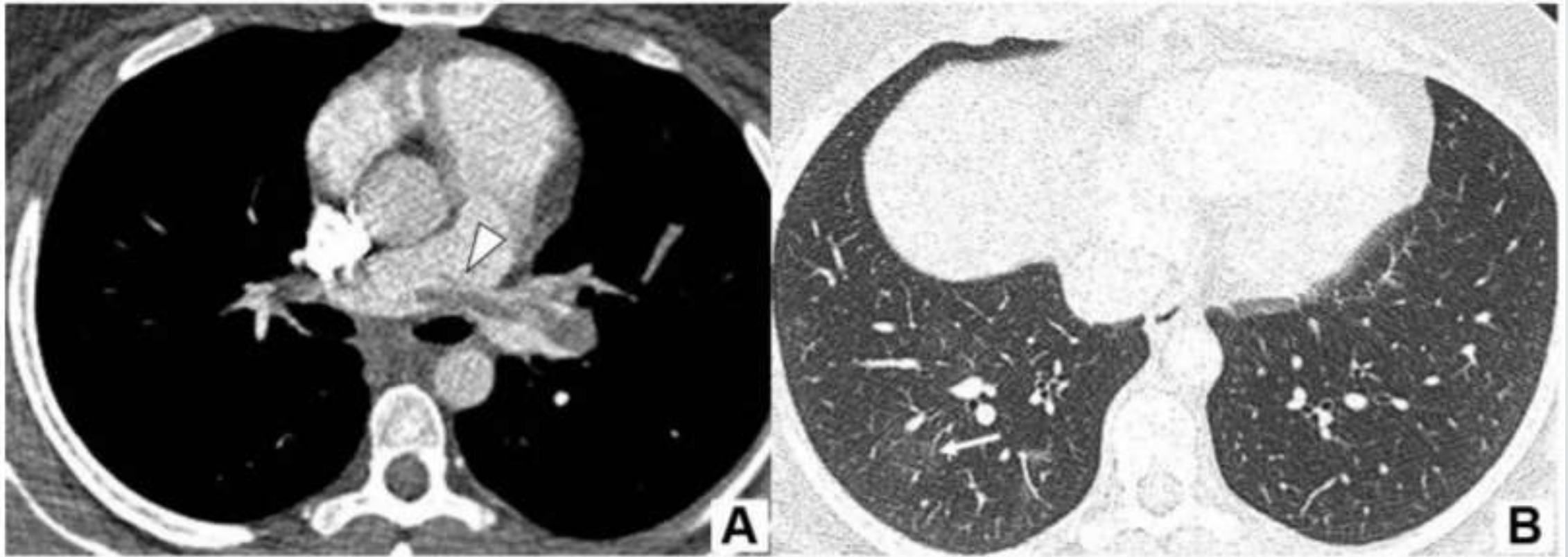
Axial image depicts fibrosis after COVID-19 in a 79-year-old woman. CT obtained 3 months after acute infection with acute respiratory distress syndrome shows reticular abnormality with traction bronchiectasis. Mild patchy ground-glass opacity is also present. Findings were new from CT scan prior to COVID-19, and patient had persistent exertional dyspnea.



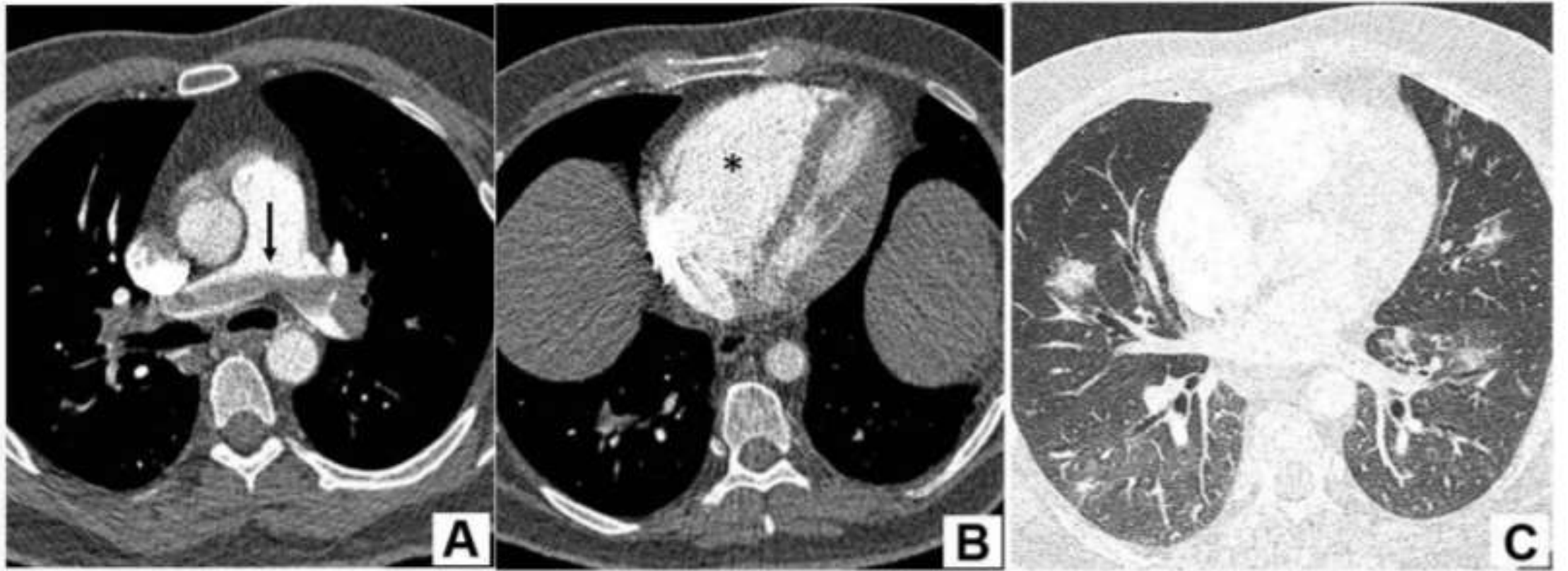
Images show progressive fibrosis following COVID-19 in a 64-year-old man. Patient had a relatively mild COVID-19 infection that did not require intensive care unit care, but subsequently developed progressive shortness of breath. (A) Axial CT obtained 6 weeks after infection shows moderately extensive reticular abnormality with traction bronchiectasis. (B) Axial CT obtained 6 months later shows progressive reticular abnormality and traction bronchiectasis. Patient had progressive shortness of breath and physiologic impairment.



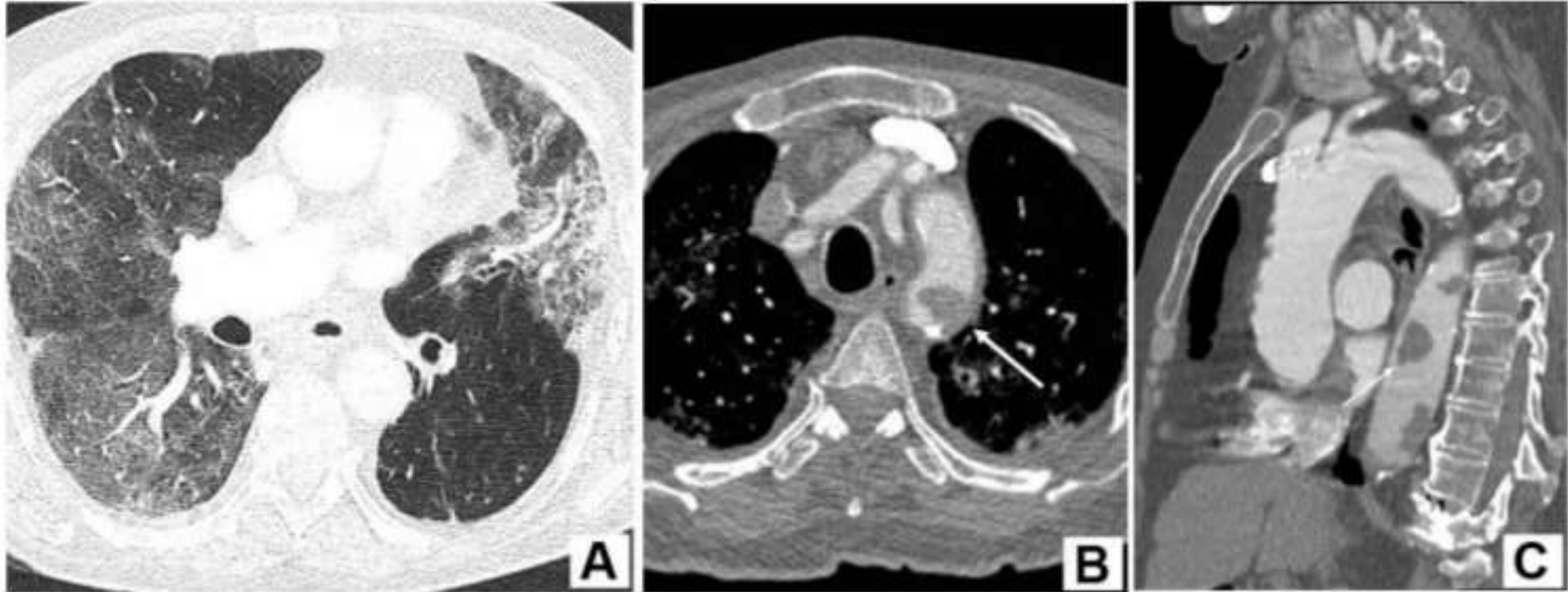
: A 49-year-old man, obese, with COVID-19 pneumonia, presents sudden onset of dyspnea and elevated D-Dimer. CT angiography of the chest, lung window (a and b) and mediastinum (c); evidence of right unilateral pulmonary thromboembolism (arrowhead), pneumomediastinum (*), subcutaneous emphysema (black arrow), minimal left pneumothorax (white arrow) and multifocal bilateral ground-glass opacities with pulmonary involvement around 50%.



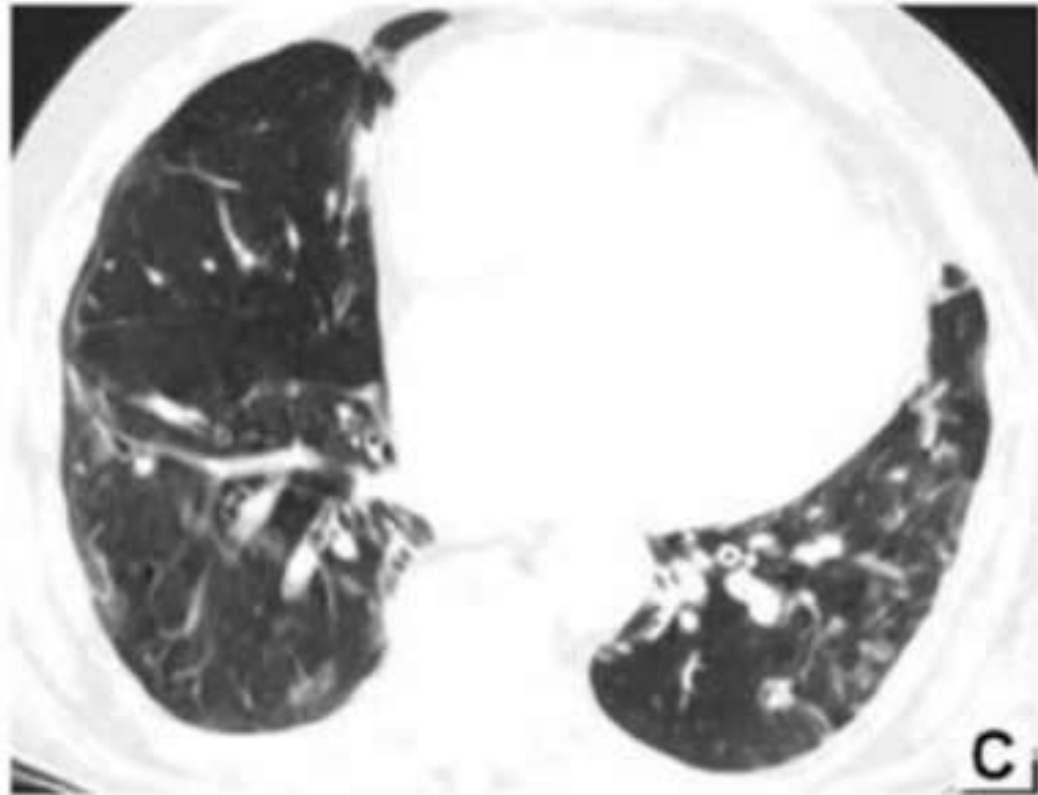
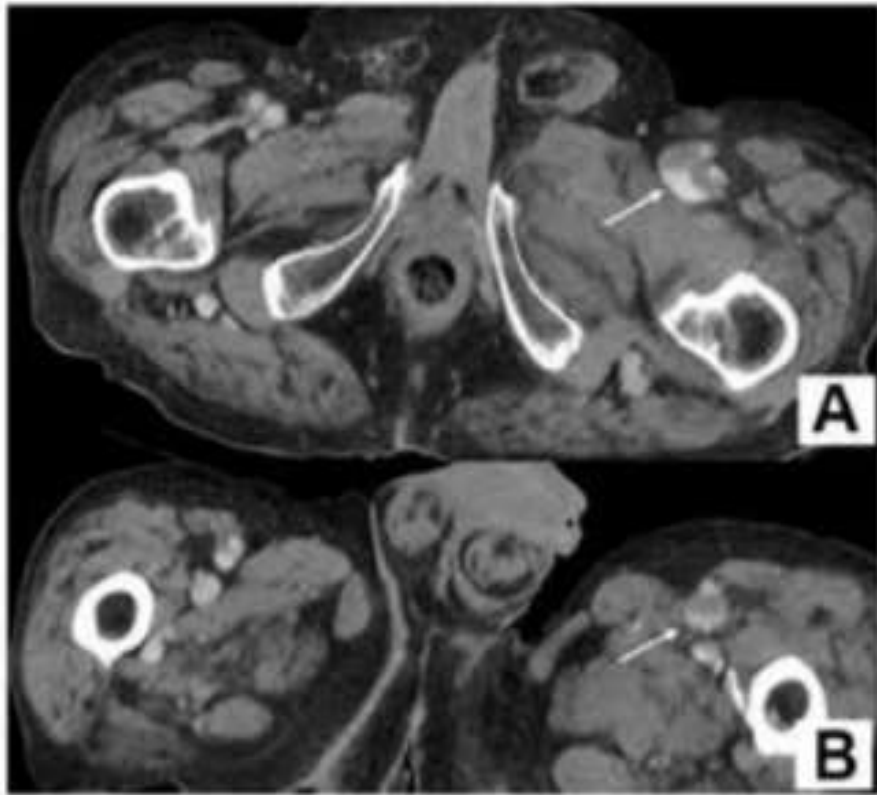
26-year-old woman with a history of oral contraceptive treatment, symptoms of dry cough and dyspnea (suspected COVID-19 infection), sinus tachycardia, S1Q3T3 ECG pattern and D-Dimer elevation. CT angiography of the chest, mediastinum (a) and lung (b); evidence of bilateral pulmonary embolism with saddle thrombus (arrowhead) and right chamber overload. Faint bilateral ground-glass opacities with pulmonary involvement in around 25% (arrow).



A 50-year-old man with cardiovascular risk factors and chronic liver disease presents with a one-week history of cough, mid-thoracic pain, anatomic symptoms, and elevation of the D-Dimer. CT angiography of the chest, mediastinum (a, b) and lung (c); evidence of bilateral pulmonary embolism with saddle thrombus (arrows) and right chamber overload (). Bilateral ground-glass opacities with pulmonary involvement around 25%.*



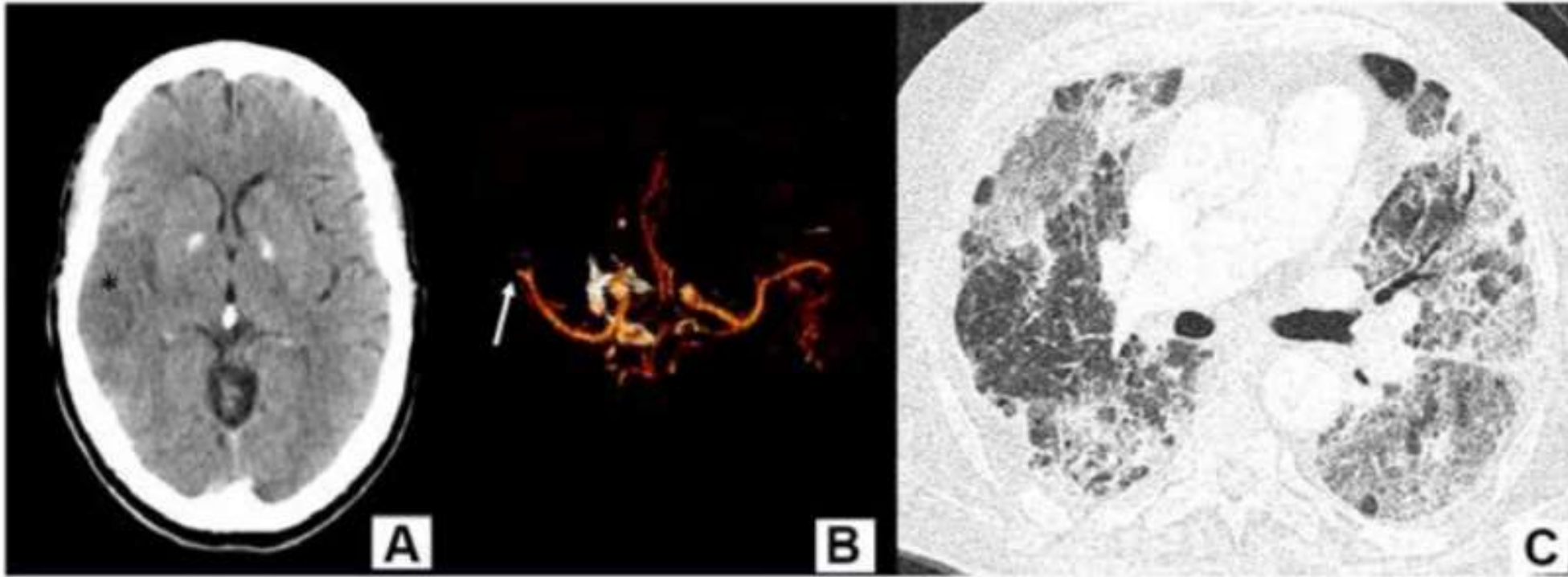
89-year-old male diagnosed with COVID-19 with a torpid progress and increased D-Dimer. CT angiography of the chest, lung window (a); Ground-glass opacities with 50-75% involvement of the lung parenchyma. Mediastinal window axial slice (b) and coronal (c) floating thrombi in aortic arch and descending thoracic aorta (arrows).



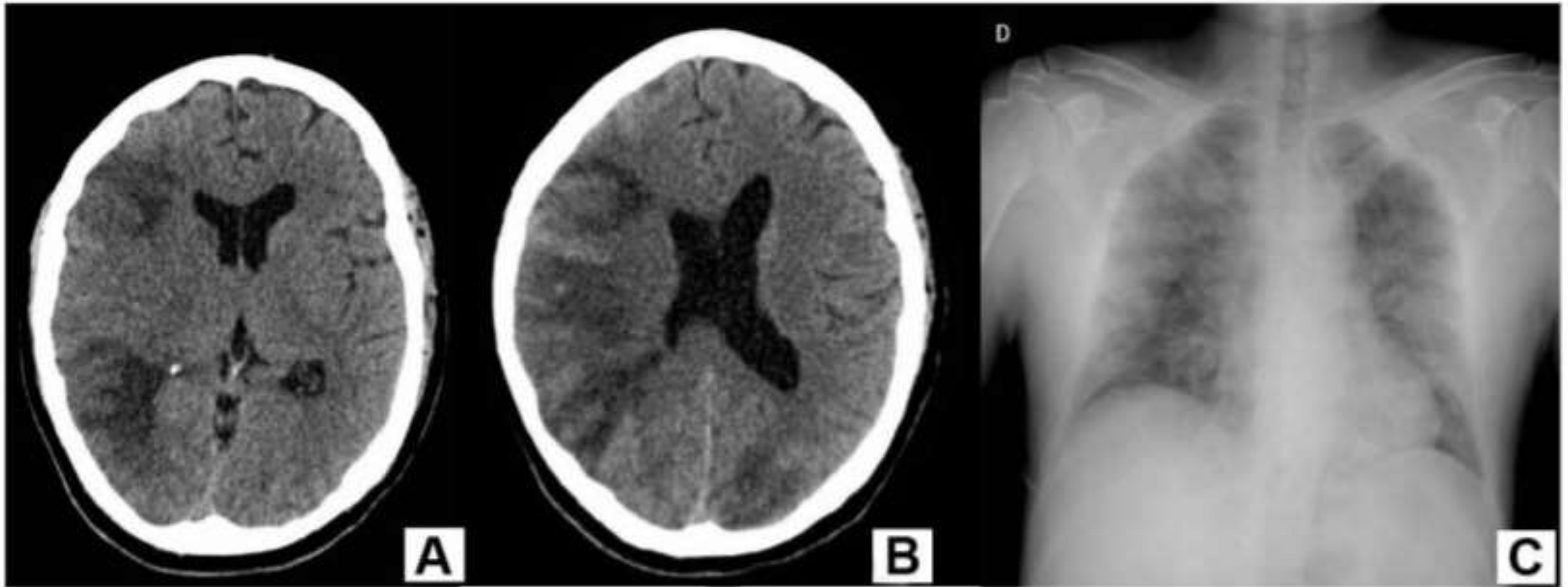
: 77-year-old man diagnosed with COVID-19 with a torpid progress and increased D-Dimer. Abdominopelvic CT with iv contrast (a.) Filling defect of the common, superficial and deep femoral veins, in relation to DVT. (arrows). Chest CT, lung window (b); Ground-glass opacities with pulmonary involvement around 25%.



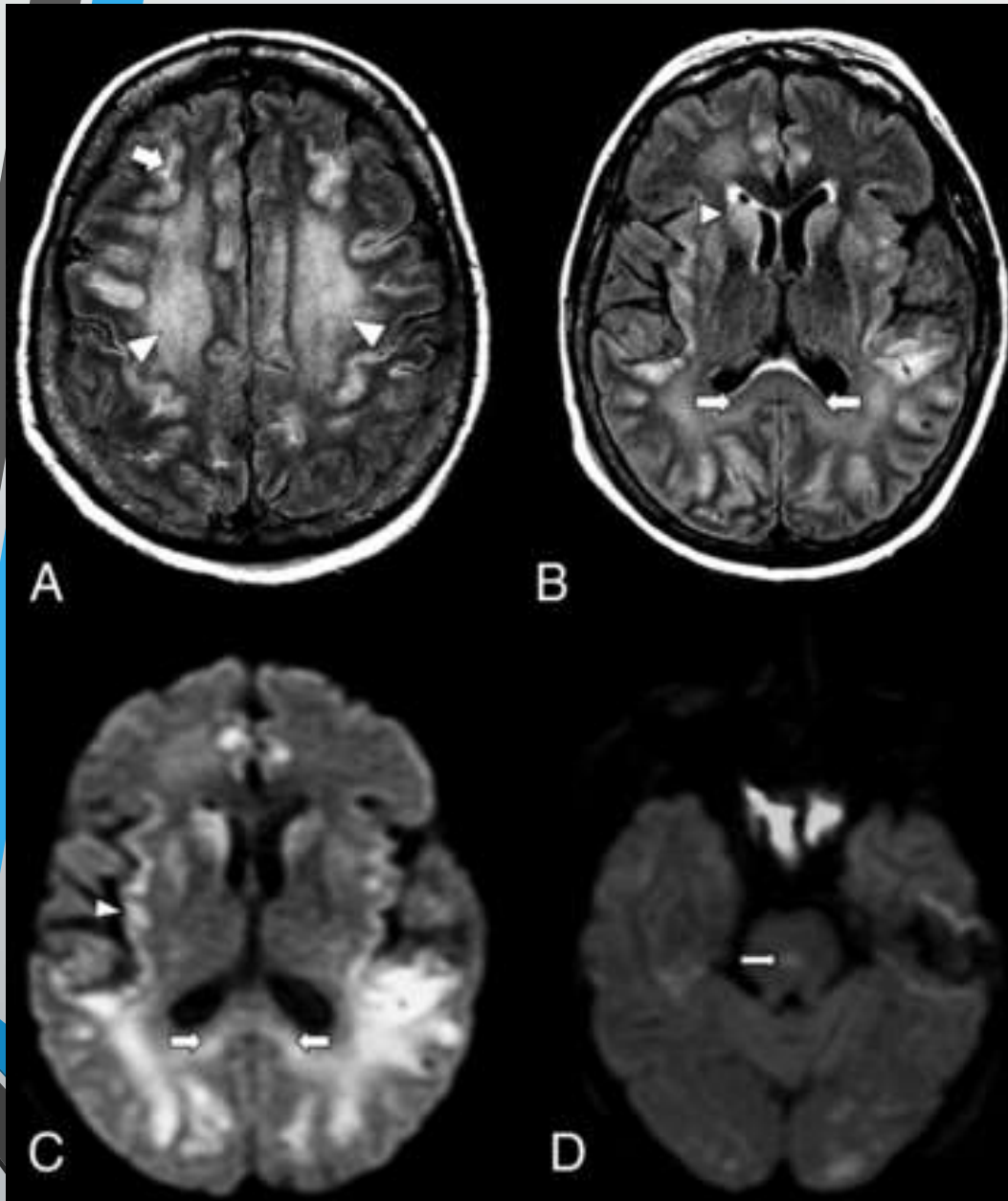
48-year-old woman with no relevant history with symptoms of dry cough and dyspnea (suspected COVID-19 infection) and elevated D-Dimer. Chest CT angiography, mediastinal window (a.) Shows a filling defect in the right anterior and internal jugular vein compatible with thrombosis (arrows). Lung window (b); predominantly multiple parenchymal consolidations are seen in RLL.



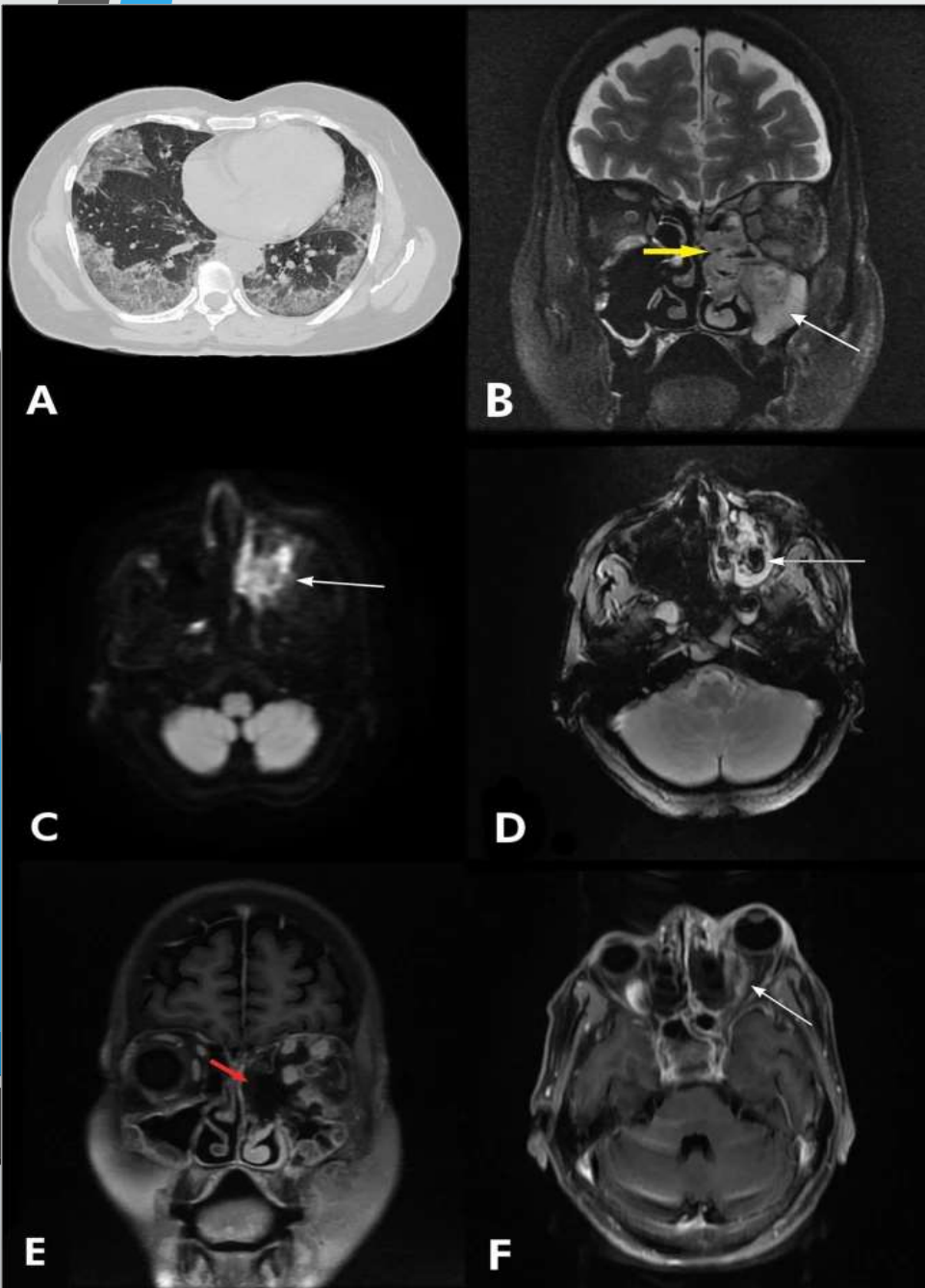
A 77-year-old man with COVID-19 pneumonia presents symptoms of facial and left brachial paresis. Cranial CT without iv contrast (a). Hypodense cortical subcortical lesion in the right cerebral hemisphere compatible with acute ischemia in the territory of the right middle cerebral artery (*). CT with iv contrast, Willis polygon with 3D reconstruction (b) shows obstruction of the right M2 segment (arrow). Chest CT lung window showing extensive areas of bilateral ground-glass and cobblestone pattern.



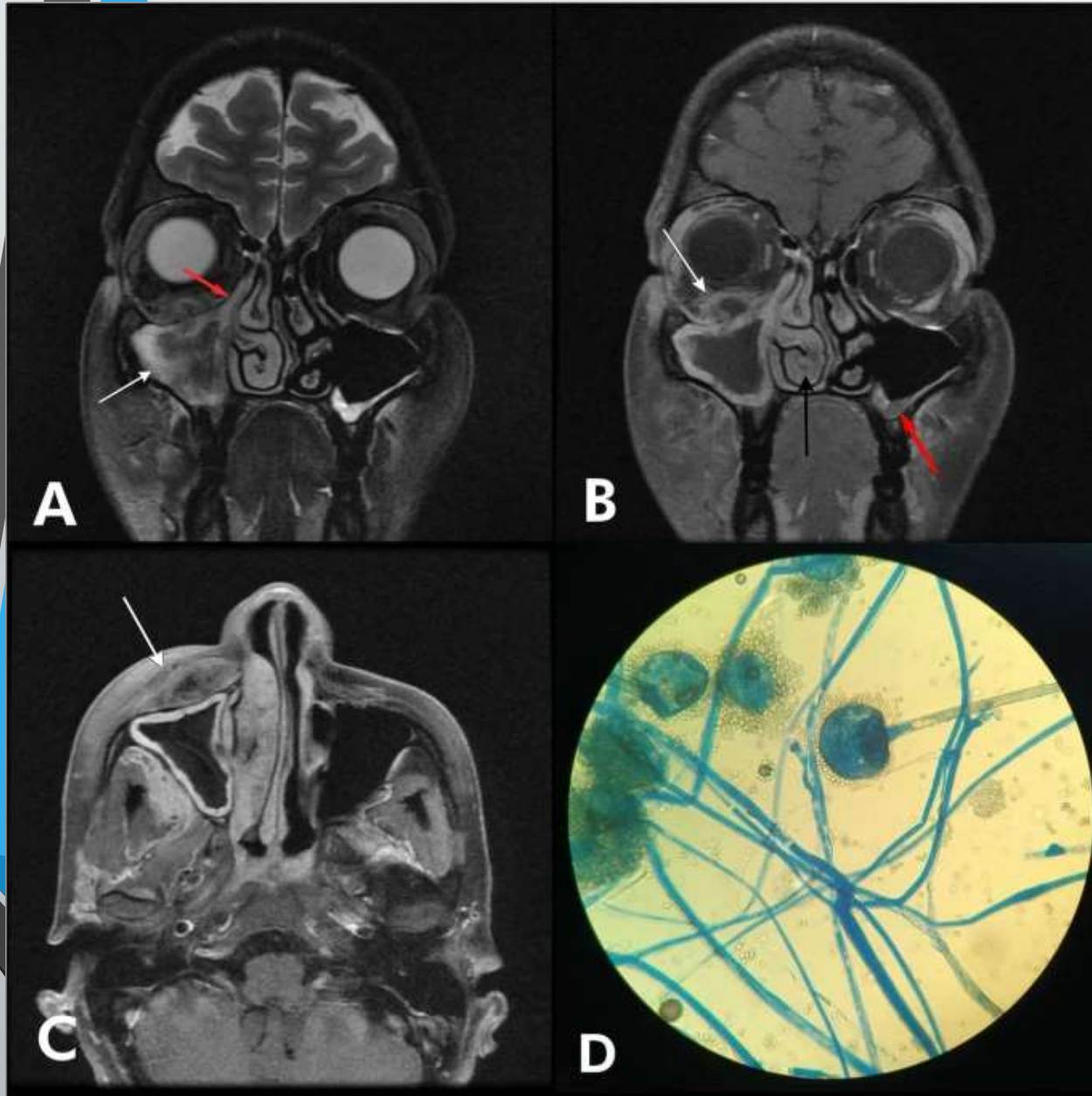
56-year-old male, SARS-CoV-2 positive, admitted to the ICU due to severe respiratory failure, after removal of sedation, left hemiparesis with asymmetric reflexes was clear. Cranial CT without iv contrast (a and b). Ischemic lesion in the territory of the right middle cerebral artery and left posterior cerebral artery. PA chest radiograph (c) shows bilateral peripheral patchy opacities in both hemithorax.



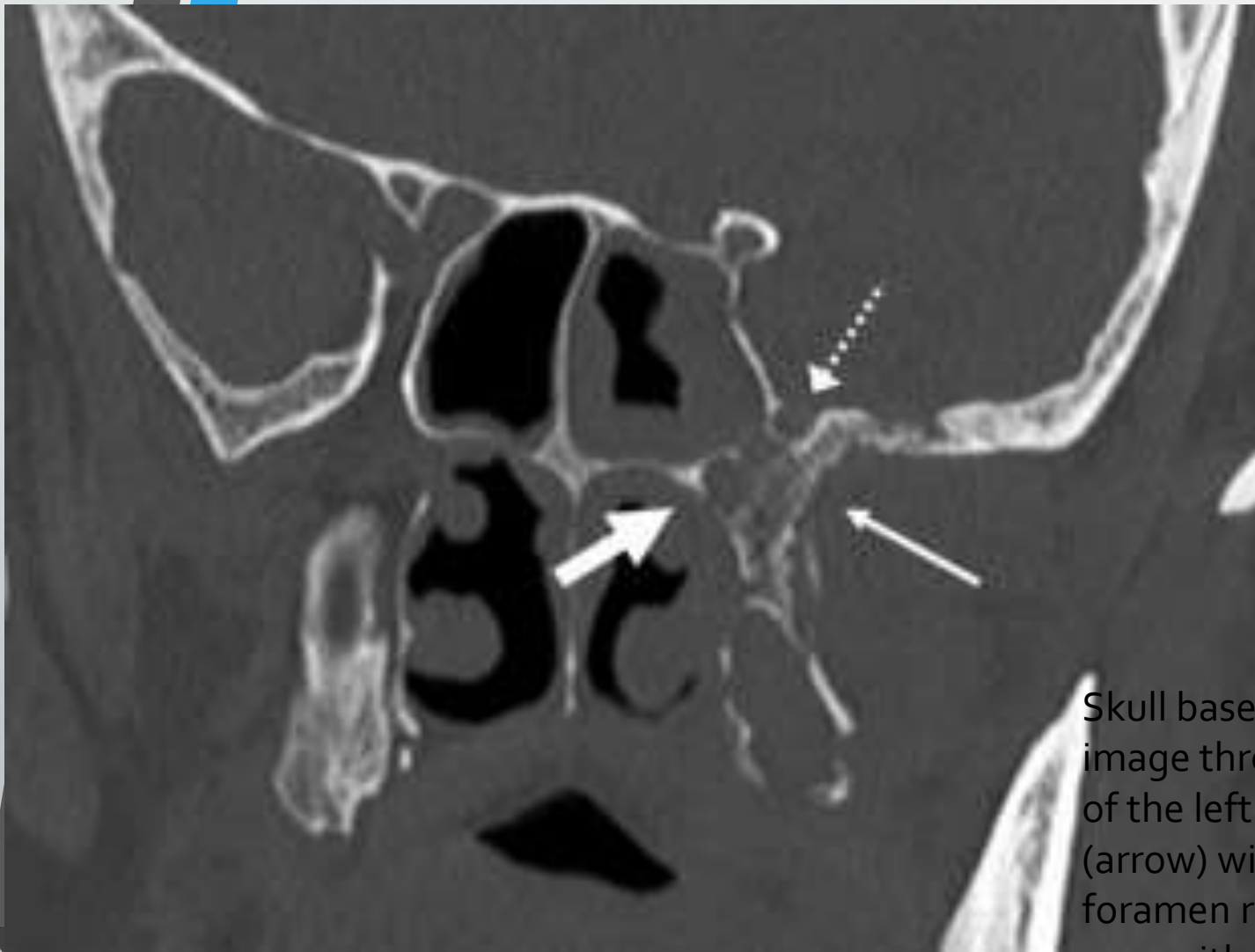
An axial MR image of a 59-year-old woman with COVID-19 who presented with respiratory distress and acute disorientation (case 1). A, FLAIR image demonstrates confluent FLAIR hyperintensity that involves cerebral WM (arrowheads) and patchy involvement of cerebral cortices; a small amount of scattered frontoparietal leptomeningeal FLAIR hyperintensity is noted (arrow). B, FLAIR image shows hyperintensity that involves the splenium (arrows) and basal ganglia (arrowhead). C, DWI demonstrates restricted diffusion that involves the splenium of the corpus callosum (arrows) and the cortex (arrowhead). D, DWI shows a diffusion-restricting focus in the pons (arrow).



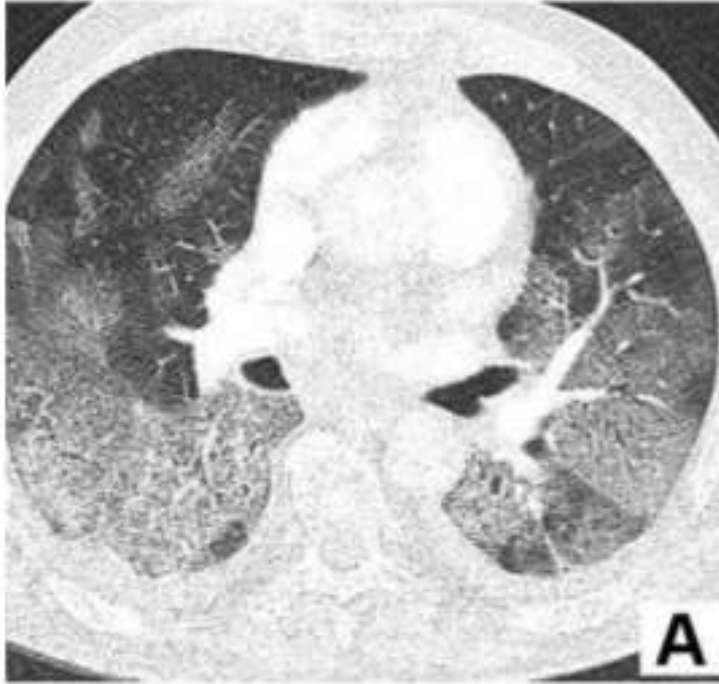
Axial HRCT thorax image showing ground-glass opacities in subpleural regions of bilateral lung parenchyma with "crazy paving appearance." b Coronal T2 FS image showing mucosal thickening and collection in the left maxillary sinus (white arrow), left ethmoidal sinus, and left middle nasal turbinate (yellow arrow) with inflamed extraocular muscles. c Axial DWI image showing restricted diffusion in the left maxillary sinus and left middle nasal turbinate. d Axial GRE image showing foci of blooming in the left maxillary sinus (white arrow). e Coronal T1 post-contrast image showing area of non-enhancing soft tissue in left middle nasal turbinate and within the left maxillary antrum ("black turbinate sign"). f Axial T1 post-contrast image showing enhancement and inflammation involving extraocular muscles of left orbit causing proptosis



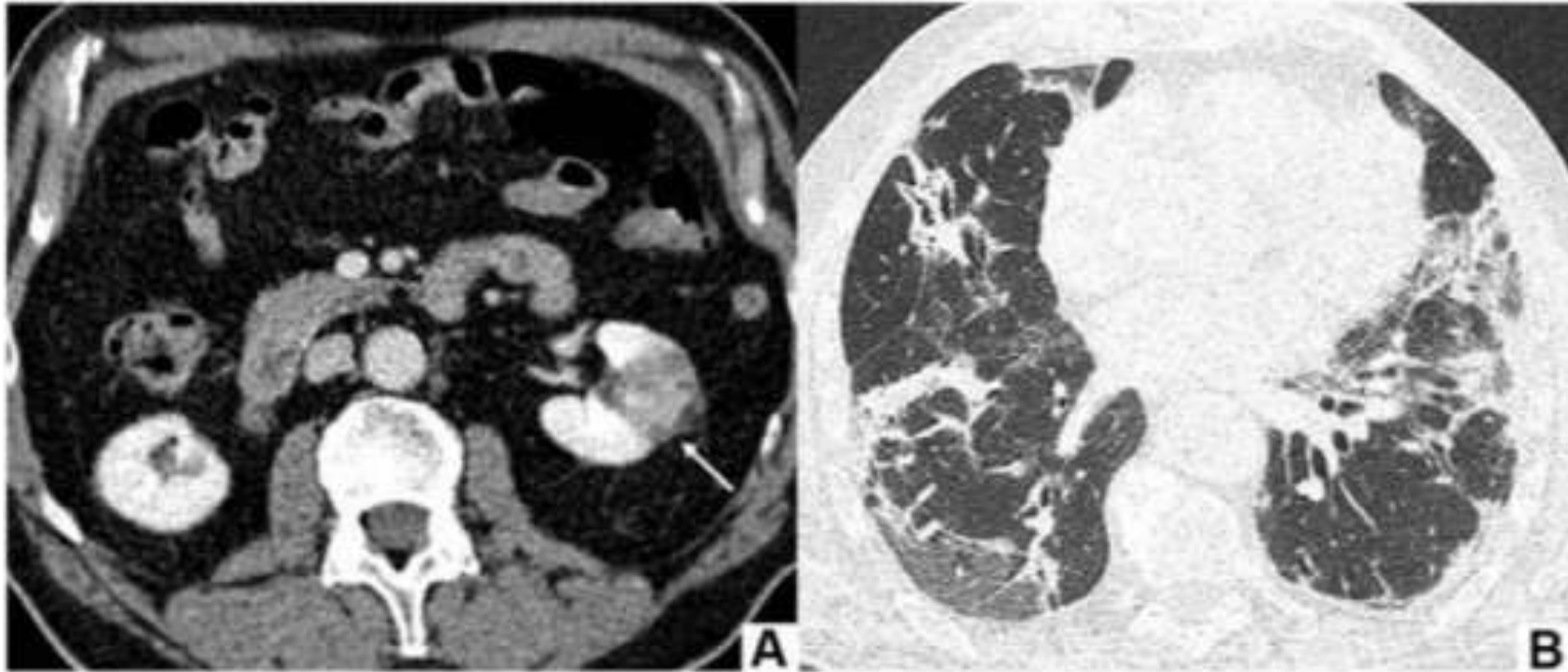
Coronal T2 image showing mucosal thickening in right maxillary sinus (white arrow) causing blockage of the right osteomeatal unit (red arrow). b Coronal T1 FS post-contrast image showing extension of inflammation in right inferior orbit (white arrow) with post-contrast peripheral enhancement, right inferior turbinate hypertrophy (black arrow), and left maxillary wall thickening (white arrow). c Axial T1 FS post-contrast image showing right pre-maxillary soft tissue swelling with enhancement (white arrow). d Lactophenol cotton blue (LPCB) stain showing broad ribbon-like fungal hyphae with sporangium



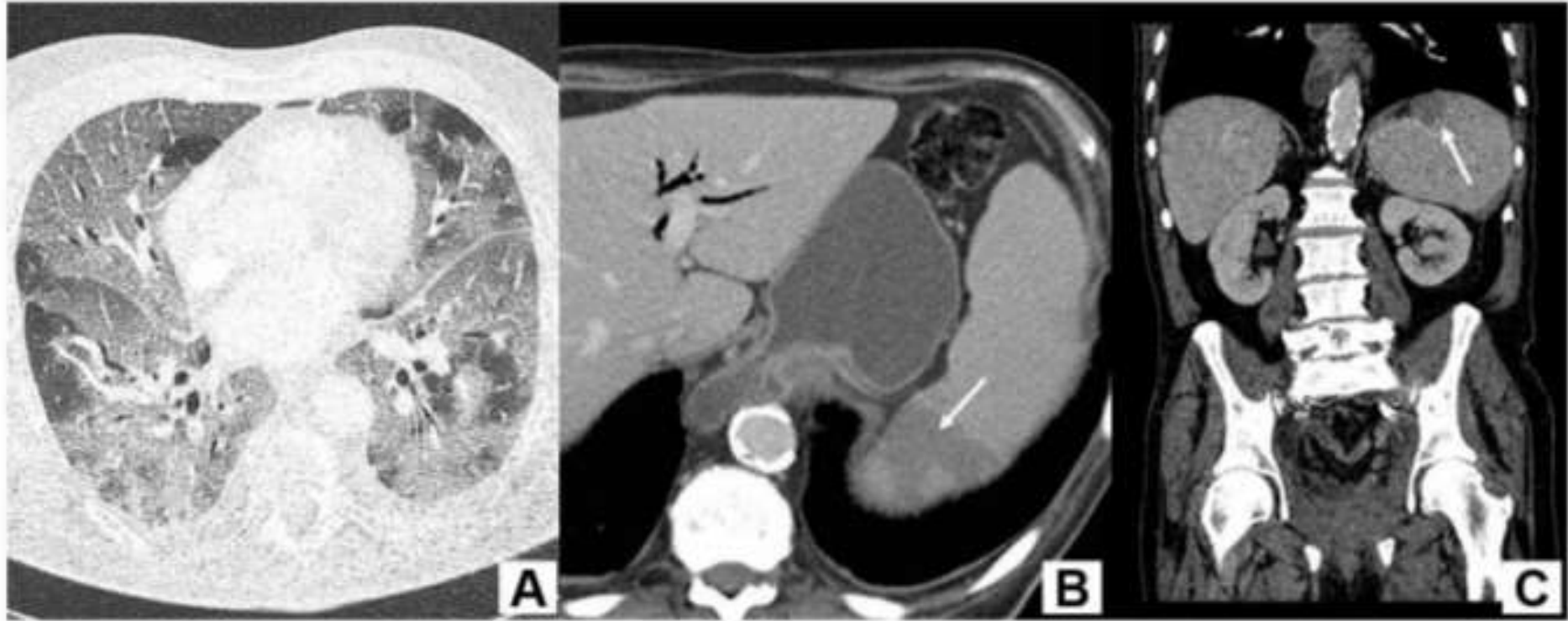
Skull base foraminal involvement. Coronal reconstructed CT image through the central skull base shows bony destruction of the left pterygoid plates and sphenoid body/greater wing (arrow) with involvement of the vidian canal (thick arrow) and foramen rotundum (dotted arrow). A 65-year-old, diabetic man with loosening of the teeth, facial pain, and severe headache. Treated for COVID-19 with injectable corticosteroids and mechanical ventilation. Duration between RT-PCR positivity and first maxillofacial imaging was 21 days.



70-year-old man with COVID-19 lung involvement, presents with acute abdominal pain, rectal bleeding, increased CRP and D-dimer. Abdominal CT with iv contrast, lung window in the middle fields shows extensive and bilateral ground-glass involvement predominantly posterior. Section at the level of the mesogastrium (b) and coronal MPR reconstruction (c) shows circumferential thickening of the wall of the left colon with increased attenuation of the adjacent fat suggestive of ischemic colitis.



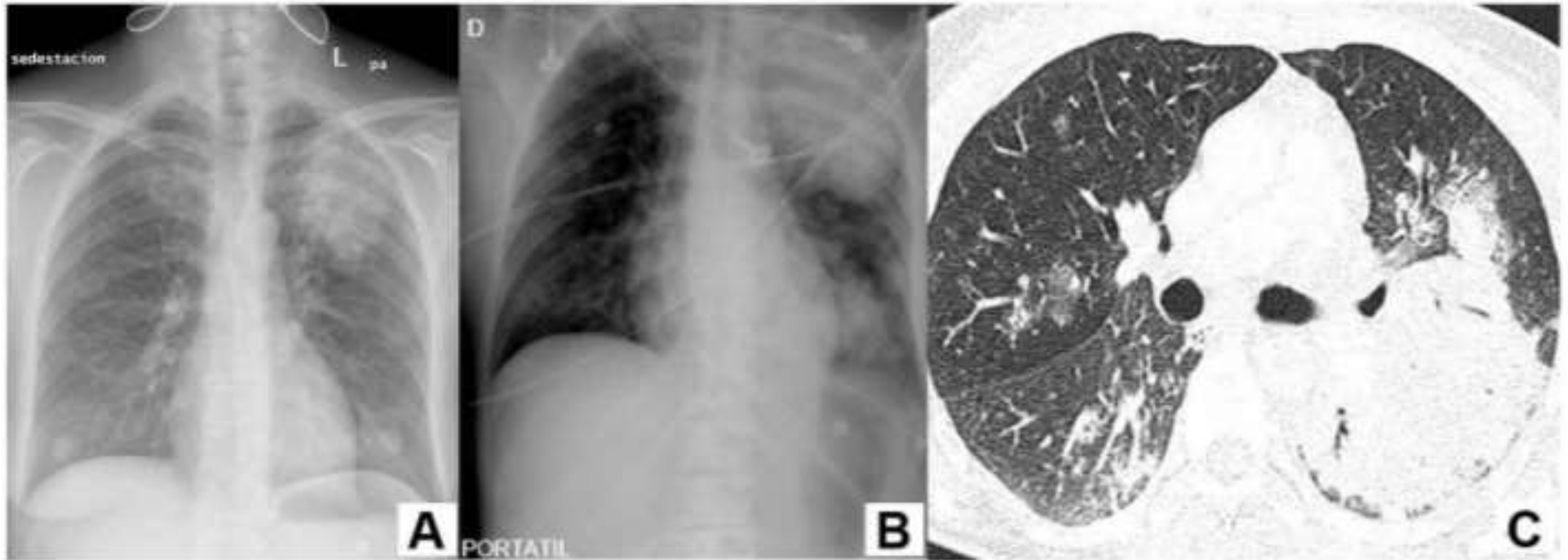
A 78-year-old man with pulmonary involvement due to COVID-19, presents with acute abdominal pain, impaired kidney function and elevated D-Dimer. Abdominal CT with iv contrast (a). Left renal infarction (arrow). Lung window at the level of the lower fields shows a cobblestone pattern, subpleural bands and bronchiectasis.



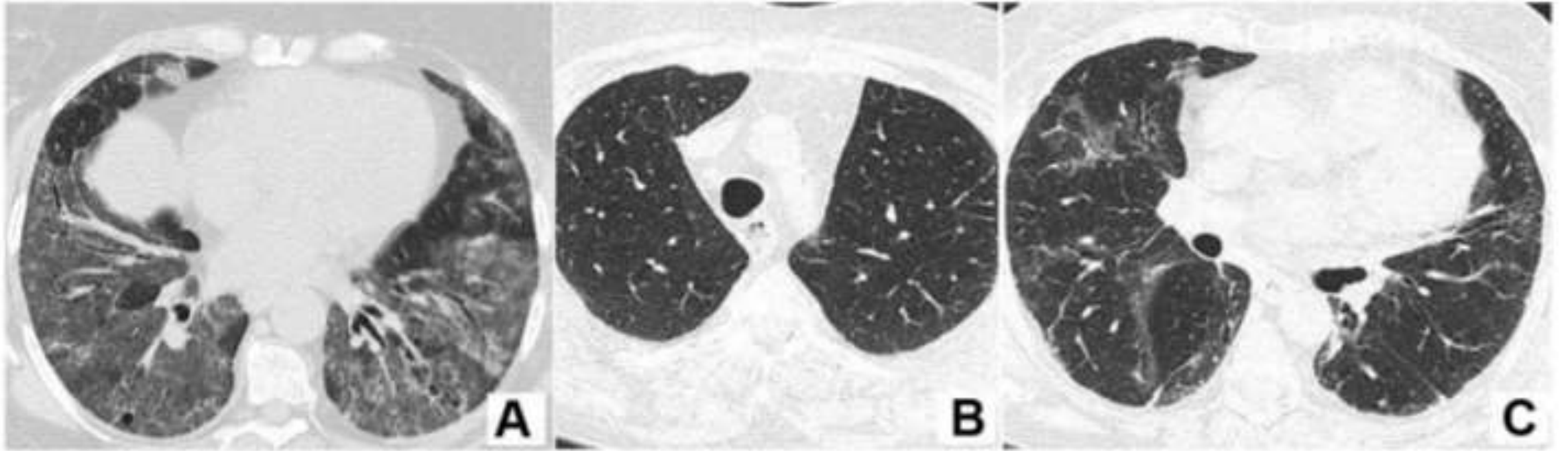
A 70-year-old man with COVID-19 parenchymal involvement, presents with acute abdominal pain, fever, and D-Dimer elevation. Abdominal CT with iv contrast. Middle field lung window shows extensive and bilateral ground-glass involvement. Soft tissue window section in the upper hemiabdomen (b) and coronal MPR reconstruction (c) showing splenic triangular hypodensity compatible with infarction (arrow).



A 57-year-old woman with a history of AF, admitted for pulmonary involvement due to COVID-19 and anticoagulant treatment for right DVT, presents with hypotension and a decrease of 4 mg / dl in hemoglobin. Abdominal CT with iv contrast (a). Extensive hematoma of the left psoas () with increased attenuation of retroperitoneal fat. Lung window in middle fields (b) showing predominantly peripheral pulmonary consolidation in both lower lobes and patchy areas of ground-glass density. Arteriography pre (a) and post-embolization (b) of active bleeding of the left distal lumbar artery and iliopsoas artery (Arrows).*



48-year-old woman with symptoms of fever, dyspnea and mild hemoptysis, peripheral blood smear compatible with acute leukemia. PA chest x-ray on admission (a) shows LUL and retrocardiac opacities. Portable control chest X-ray at 1 hour (b) shows radiological worsening. Chest CT, lung window (c), shows ground-glass opacities and consolidation. Interlobular septal thickening is not observed. Finding compatible with acute diffuse alveolar hemorrhage, given the clinical context.



Woman with polymyositis and diagnosis of NSIP under treatment with corticosteroids, consultation for cough without dyspnea (suspected SARS-CoV-2 infection). Previous lung CT from December 2018, without iv contrast. Lung window in lower fields (a) Fine reticular pattern and ground-glass with basal distribution without fibrotic component. Lung CT at entry to the level of upper (b) and lower (c) fields, discrete reticular pattern probably residual and inconclusive for COVID-19, with preservation of upper fields.



57-year-old woman with a history of infiltrating ductal carcinoma of the right breast and carcinomatous lymphangitis. CT angiography of the chest, mediastinal window (a) and lung window (b) shows nodular fissure thickening (arrowhead) and interlobular septa, ground-glass opacities or consolidation (*) with a right unilateral distribution. Bilateral pleural effusion is also seen (Arrow).

Thanks for your attention

